Local time-dependent magnetization of superconducting films in the presence of a transport current

M. McElfresh
Physics Department, Purdue University, West Lafayette, Indiana 47907

E. Zeldov
Department of Condensed Matter Physics, Weizmann Institute of Science, Rehovot 76100, Israel

John R. Clem
Ames Laboratory–U.S. Department of Energy and Department of Physics and Astronomy, Iowa State University, Ames, Iowa 50011

M. Darwin, J. Deak, and L. Hou
Physics Department, Purdue University, West Lafayette, Indiana 47907
(Received 8 August 1994; revised manuscript received 12 December 1994)

The time dependence of the normal component of the local flux density $B_z(t)$ was studied using a small Hall sensor placed on a thin film of the high-temperature superconductor $YBa_2Cu_3O_7$. Following the preparation of the critical state, the time dependence of $B_z(t)$ was studied before, during, and after the application of both positive and negative transport currents. Initial application of current results in an increased relaxation rate. A simple approximation for the relaxation behavior was used to calculate the spatial dependence of the current and flux densities as a function of time using a modified Bean critical-state model that incorporates demagnetization effects in superconducting films. With this model it was possible to account for most of the observed behavior.

I. INTRODUCTION

The characteristics of current-carrying superconducting films are of interest not only for fundamental reasons but also because of their importance to potential device applications. Such films have been studied using numerous experimental methods. The recent development of miniature Hall probes,[1] for example, has made it possible to investigate the dynamics of magnetic flux penetration into superconducting films with unprecedented detail, and in this paper we take advantage of this technique.

Recently, we reported results that used microscopic Hall sensors to study the effects of transport currents on the flux distribution in high-temperature superconducting $YBa_2Cu_3O_7$ (YBCO) thin films.[2] These results described some anomalous effects associated with the application and removal of a transport current in a thin superconducting film initially in the critical state. These effects could be accounted for by considering the role of demagnetization on the distribution of currents in thin film samples. A theoretical method for treating demagnetization effects was also described briefly.

More recently, we presented the basic ideas and fundamental equations needed for a detailed understanding of the critical-state current-density and magnetic-field distributions in thin films subjected to slowly time-varying transport currents and perpendicular applied magnetic fields.[3] There we considered distributions of the magnetic flux density $B_z(x)$ normal to a superconducting strip of width $2W$ along the x direction, infinite length along the y direction, and thickness d along the z direction ($d \ll W$). We treated the case for which the critical current density J_c is a constant (independent of x and B), such that the magnitude of the current density $J_y(x)$ is equal to J_c in a region of the sample in which $B_z(x)$ had just changed. We showed that there are field-invariant regions, where $B_z(x)$ does not change so long as the magnitude of the current density $J_y(x)$ remains less than the critical current density J_c.

In Ref. 3, as in similar work by Brandt and co-workers (Refs. 4 and 5), we implicitly assumed that the electric field E is zero when the current density J obeys $|J|<J_c$, and that it obeys $|E|=\rho_f(|J|-J_c)$ for $|J|>J_c$ (which only exists for very short times immediately after changes in the applied field or transport current). A consequence of this assumption is that, depending upon prior magnetic history, the local magnetic field and current density under constant applied field and transport current quickly relax to unique, but history-dependent, distributions characterized by J_c.

An important feature of the experiments of Ref. 2, as well as those we report in this paper, is a slow relaxation, approximately logarithmic in time. Such behavior arises from the specific dependence of the electric field E on current density J, and is evident as a rounding of the $E(J)$ curve in the vicinity of J_c. Such curves are often approximated for J near J_c by $E(J)=E_c\exp[(J-J_c)/J_{th}]$, where E_c is the electric-field criterion used to define J_c, and J_{th} is a rounding parameter of thermal origin. In some models, $J_{th}=J_c kT/U$, where k is Boltzmann's constant, T the absolute temperature, and U an activation energy for flux creep. When combined with Faraday's law and Ampere's law, the exponential form of $E(J)$ generally gives rise to magnetic relaxation in which, for long times t, E varies as $1/t$, and J can be expressed as a constant plus a term that decreases as $\ln(t)$. Under these

particular conditions, for example, the exact solutions for magnetic relaxation of a thin superconducting cylindrical shell of radius R and thickness d are $E=E_c/(1+t/t_c)$ and

$$J=J_c[1-(J_{th}/J_c)\ln(1+t/t_c)]\ , \tag{1}$$

so that the field inside the cylinder decays as

$$H_i=Jd=J_cd[1-(J_{th}/J_c)\ln(1+t/t_c)]\ .$$

Here $t_c=\mu_0RdJ_{th}/2E_c$ is an L/R time constant, since the inductance of unit length of the cylinder is $\mu_0\pi R^2$ and the corresponding differential resistance is $2\pi R\rho_c'/d$, where $\rho_c'=(dE/dJ)_c=E_c/J_{th}$. The time $t=0$ corresponds to the time that $E=E_c$ and $J=J_c$.

In general, to determine the evolution with time t of the magnetic flux density $B_z(x,t)$ as well as that of the electric field $E_y(x,t)$ and the current density $J_y(x,t)$, three coupled equations involving these three functions must be solved simultaneously: Faraday's law, Ampere's law, and the equation that relates E and J, subject to the boundary conditions at the surface. Numerical solutions would be required in such a procedure.[6,7] In this paper, however, we do not solve these equations exactly, but instead make use of a simpler approach that takes advantage of known analytic solutions for a strip with a spatially dependent critical current density $J_c(x)$.[3] We account for the time dependence phenomenologically, noting from earlier work that, after the critical state is established (at time $t=0$) with a current density J_c, it relaxes approximately logarithmically with time, according to an equation similar to Eq. (1).

The organization of this paper is as follows. In Sec. II, we present new experimental results showing details of how the rate of local magnetic relaxation depends upon prior magnetic-field and transport-current history. In Sec. III, we present a theoretical framework for the description of these results, and in Sec. IV, we apply the theory to the experiments. Finally, in Sec. V, we present a brief summary of the key results of our paper.

II. EXPERIMENTAL

An epitaxial YBCO thin film, with the c-axis perpendicular to the film plane, was prepared by pulsed-laser deposition on a heated (001) $LaAlO_3$ substrate as previously described.[8] The film was about 3000 Å thick. The superconducting transition temperature (T_c) was 91 K, and the transition width ΔT_c was about 2 K as measured by ac susceptibility at 2.5 MHz. A strip about 230 μm wide and 5000 μm long was laser patterned into the YBCO film.

The normal component of the local magnetic flux density (B_z) was measured using a small single-crystal InSb Hall sensor with an active area approximately 35 μm wide and 35 μm high. The specification and operation of this type of Hall sensor have been described previously.[1,2] The Hall sensor was positioned over the superconducting strip, with the right edge of the Hall sensor approximately 35 μm to the left of the right edge of the strip and its bottom surface about 30 μm from the top surface of the strip. Magnetic fields of up to 600 Oe were supplied by a copper-wound magnet and were applied parallel to the YBCO c axis (z direction). Transport currents were applied in the y direction. The critical current density J_c was determined from magnetic J_c measurements made over the temperature range 78–90 K and transport J_c (current-voltage) measurements from 87.5 to 90 K. At $T=78$ K a value $J_c\approx2.2\times10^6$ A/cm^2 was determined, which corresponds to a critical current $I_c\approx1.6$ A.

The local magnetic flux density B_z was measured as a function of time after a preparation sequence that began by warming the strip well above T_c. The strip was then cooled in zero applied field and the temperature stabilized. Next, the field was cycled through half a hysteresis loop with the maximum applied field being large enough to place the superconductor in the remanent (trapped-flux) critical state. The time $t=0$ was defined as the time at which the applied magnetic field returned to zero. After this preparation, B_z was measured as a function of time in this remanent state ($H_a=0$) and was typically monitored for 4000 sec at a fixed temperature between 78 K and T_c. The time at which the transport current was applied was defined as t_{on}, and the time the current was removed was t_{off}.

The first type of study involved applying a series of different transport currents (I_T) during the time interval 200 s $<t<$ 2000 s. For this case, the full preparation sequence was repeated for each value of I_T. In the second type, a current I_T of the same magnitude was applied at a series of different initial times t_{on} with the current removed at the same time ($t_{off}=2000$ s). For this second case, the full preparation sequence was repeated for each value of t_{on}.

The time dependence of the local flux density $B_z(t)$ measured at $T=78$ K for different values of the applied transport current I_T is shown in Fig. 1. The results for

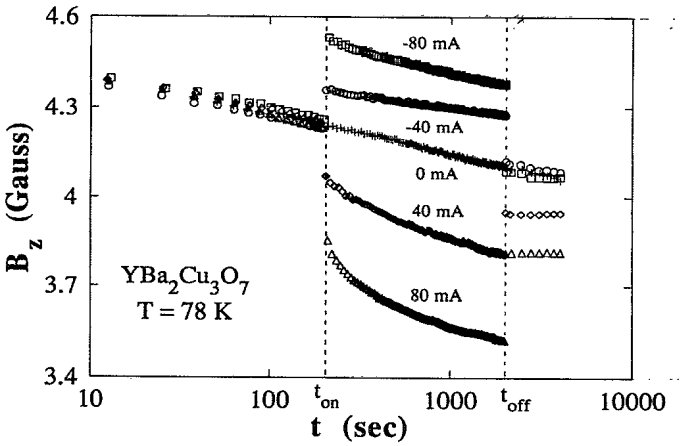

FIG. 1. Time dependence of the local magnetic flux density B_z measured by the Hall sensor for different values of applied transport current in a YBCO film at $T=78$ K. In separate runs, either positive or negative currents were applied during the time segment between t_{on} and t_{off}. Current values of 0, ±40, and ±80 mA are presented. The critical current $I_c\approx1.6$ A at $T=78$ K.

I_T values of 0, ±40 and ±80 mA are presented and show that initially the time decay is nearly logarithmic, typical of YBCO. The value $I_T=80$ mA corresponds to approximately 5% of the critical current density at $T=78$ K. Prior to the application of a transport current, all the data have approximately the same logarithmic dependence, with a slight spread of initial B_z values resulting from small variations in the preparation of the critical state. As seen in Fig. 1, when a positive I_T is applied, there is a step decrease in B_z, while for negative currents there is a step increase in B_z. There is a clear asymmetry in the shape of the curves during current application, with positive current application initially leading to large changes in the relaxation rate $dB_z/d\ln(t)$ and negative current application having only a small effect on the relaxation rate. It can also be seen in Fig. 1 that when a negative current is removed, B_z returns to nearly the same value that would be expected if the current had not been applied. This is in contrast to removal of a positive current, in which case there is a large negative offset in B_z after current removal. The steps seen at t_{on} and t_{off} are a result of several contributions, including those due to the separation of the Hall sensor from the sample surface and the finite thickness of the sensor. A plot of the size of the steps at t_{on} and t_{off} as a function of the I_T value is shown in Fig. 2.

Shown in Fig. 3 is $B_z(t)$ measured at $T=78$ K when a current of either $I_T=40$ mA or -40 mA is applied at a series of different values of t_{on}. The behavior is essentially the same as that in Fig. 1. However, it is now more apparent that application of a negative current results in a reduction of the slope $dB_z/d\ln(t)$ and that the slope during this negative-current application is essentially independent of the time t_{on}. In addition, it is more apparent from Fig. 3 that when a positive current is removed at t_{off}, a relaxation rate less than the baseline rate is observed, whereas the removal of a negative current results in an increased relaxation rate.

III. THEORETICAL MODEL

We now model the effects of relaxation on the distributions of magnetic flux density and electric currents. The

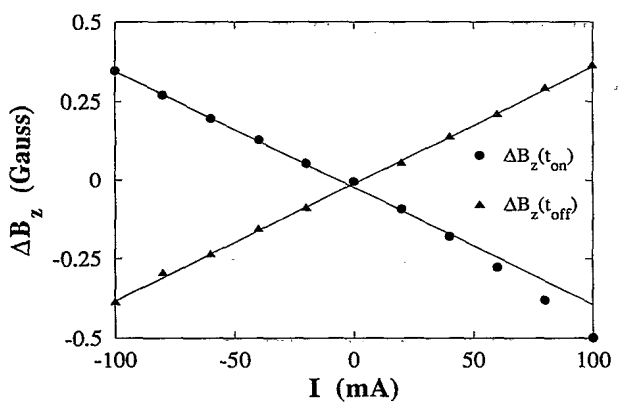

FIG. 2. The change in local magnetic flux density ΔB_z for a YBCO film at $T=78$ K at the time when the current is applied $[\Delta B_z(t_{on})]$ and when the current is removed $[\Delta B_z(t_{off})]$.

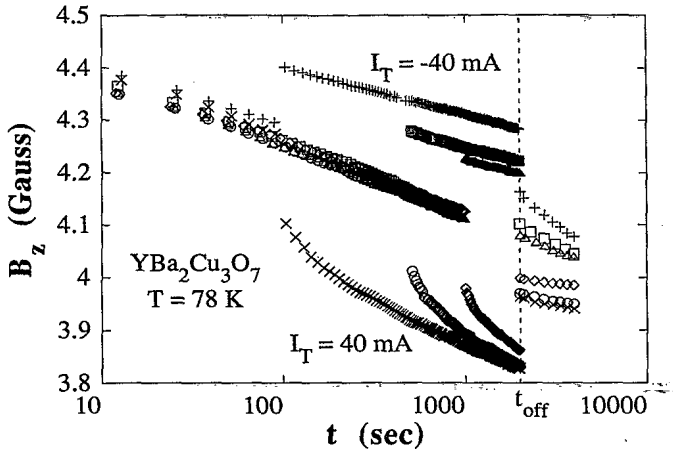

FIG. 3. Time dependence of the local magnetic flux density B_z for a YBCO film at $T=78$ K when a transport current $I_T=\pm40$ mA is applied at different values of t_{on}. The current was removed at the same time $t_{off}=2000$ s.

static current and field distributions in a thin-film strip carrying a transport current in the presence of an applied field have been calculated recently in Refs. 2–5. We now extend this approach to include the effects of relaxation. In particular, we treat the case relevant to the described experiment, namely application of transport current to a sample in a fully penetrated remanent state.[2,3]

As discussed in the introduction, the magnetic-field, current-density, and electric-field distributions, in principle, should be solved by combining Faraday's law, Ampere's law, and the E versus J relation, as in Refs. 6 and 7. Here, however, we are not interested in the rapid, transient response of the superconductor immediately following changes in the applied field or transport current. During the period τ just after the change, the electric field E is much larger than E_c, the electric-field criterion for definition of the critical current density, and the current density J is much larger than the critical current density J_c.[9] Instead, we are interested in the behavior at times t much larger than τ and t_c, for which E decreases below E_c, and J relaxes to values below J_c. We consider behavior following a change of applied field or transport current at which certain regions of the sample have just undergone changes in the local flux density, where J at time $t=0$ is equal to J_c. By ignoring transient effects ($t\gg\tau, t\gg t_c$), we can then use the simple approximation that in these regions the magnitude of the local current density subsequently relaxes with time as

$$J_c^*(t)=J_c\left[1-\frac{J_{\rm th}}{J_c}\ln(t/t_c)\right]. \tag{2}$$

We shall refer to $J_c^*(t)$ as the time-dependent critical current density, which is reestablished in any region where B_z changes after each change in either the applied field or transport current. Using this phenomenological time-dependent critical current density, we are able to calculate the relaxation of $J_y(x,t)$ and $B_z(x,t)$ in the entire sample without the need to analyze the local electric field E.

For an infinite slab in a parallel field, the critical state is determined by $|J_y|=J_c$ in the outer regions closer to the surface and by $J_y=0$ in the central field-free region of the sample. In a thin film, however, the situation is complicated by demagnetization effects, which result in a continuous current distribution throughout the sample. In this case vortex distributions may also relax in the regions where $|J_y|<J_c$. However, since the local hopping of vortices depends exponentially on the local current density, the considerably lower vortex relaxation rates in the low-current-density regions are neglected in this model. We also neglect the possible dependence of the relaxation rate on the local vortex density.

Immediately after the remanent state is established ($t=0$) in a thin film, a uniform current flows in the film with $J_y(x)=-J_c$ for $-W<x<0$ and $J_y(x)=J_c$ at $0<x<W$. We assume that for times $t\gg\tau$ this current decays with time away from the critical state according to Eq. (2). At $t=t_{\rm on}$, just prior to the application of the transport current, the time-dependent critical current density $J_c^*(t)$ has decayed to $J^{\rm on}$, as shown by curve a in Fig. 4.

In order to describe the current-density distribution in the film in the relaxed remanent state in the presence of the transport current, we use the "spatial variation of the critical current" approach developed in Ref. 3. Since $J_y(x)$ has relaxed from $t=0$, application of a positive current can now increase the current density for all values of x. At $t=t_{\rm on}$ the maximum current density increase possible, or the "available" current density J_y', for a positive transport current in the y direction is

$$J_y'(x,t_{\rm on})=J_c-J_y(x,t_{\rm on})=\begin{cases}J_c+J^{\rm on}\equiv J_L(t_{\rm on}), & -W<x<0\ ,\\ J_c-J^{\rm on}\equiv J_R(t_{\rm on}), & 0<x<W\ .\end{cases}\tag{3}$$

Applying the transport current at $t\geq t_{\rm on}$ results in a new current density distribution which is a superposition of the relaxed remanent-magnetization current density just prior to $t_{\rm on}$, $J_y(x,t_{\rm on})$, and the changes in the current-density distribution $J_y'(x,t)$. The added current at the edges takes full advantage of the available current density. Therefore, the added transport current density is given by

$$J_y'(x,t)=\begin{cases}J_L(t), & -W<x\leq p-a\ ,\\ \dfrac{1}{\pi}\left[J_R(t)\arcsin\dfrac{(x-p)(W-p)-a^2}{a(W-x)}-J_L(t)\arcsin\dfrac{(x-p)(W+p)+a^2}{a(W+x)}\right]+\dfrac{1}{2}[J_L(t)+J_R(t)]\ , & p-a<x<p+a\ .\\ J_R(t), & p+a\leq x<W\ ,\end{cases}\tag{4}$$

where p is the center of the $2a$-wide region of the film in which the field does not change (field-invariant region) as a result of the new current distribution.[3] Curve b (long dash) in Fig. 4 shows the total current distribution immediately after the transport current of $I_T=0.25I_c$ has been applied ($I_c=2WdJ_c$). Close to both edges the current density now equals J_c, and in these regions the vortex density and the field distribution inside the film are affected by the transport current. At the right edge $B_z(x)$ has decreased and at the left edge the field has increased, as shown by curve b (long dash) in Fig. 5(a). In the central region ($p-a<x<p+a$), however, B_z remains invariant. There are two conditions that determine the time-dependent width $2a$ and the time-dependent position of the center p of the field-invariant region, which appear in Eq. (4). The first comes from the fact that $J_y'(x,t)$ has to carry the externally applied transport current I_T. Integrating Eq. (4) over the width of the film and equating it to I_T, we obtain

$$I_T=d[J_R(t)\sqrt{(W-p)^2-a^2}+J_L(t)\sqrt{(W+p)^2-a^2}]\ ,\tag{5}$$

The second condition is the field invariance in the central region. In other words $J_y'(x,t)$ must have zero contribution to B_z in this region. Using the Biot-Savart formula and integrating over the width of the film (see Ref. 3), we obtain

$$\sqrt{(W-p/a)^2-1}+\frac{W-p}{a}=\left[\sqrt{(W+p/a)^2-1}+\frac{W+p}{a}\right]^{J_L(t)/J_R(t)}\ .\tag{6}$$

As the current density near the edges of the film decays from J_c, the width of the field-invariant region decreases and the center of the field-invariant region (p) shifts to the left. While Eqs. (3)–(6) are valid for any time dependence of $J_c^*(t)$, we use the logarithmic approximation of Eq. (2) for simplicity. Hence, after the transport current is applied, the total current density close to the edges decays according to Eq. (2) with t being replaced by $t-t_{\rm on}$ and as a result the added current densities at the edges relax as

$$J_L(t)=J_c\left[1-\frac{J_{\rm th}}{J_c}\ln\left[\frac{t-t_{\rm on}}{t_c}\right]\right]+J^{\rm on}\ ,\qquad J_R(t)=J_c\left[1-\frac{J_{\rm th}}{J_c}\ln\left[\frac{t-t_{\rm on}}{t_c}\right]\right]-J^{\rm on}\ .\tag{7}$$

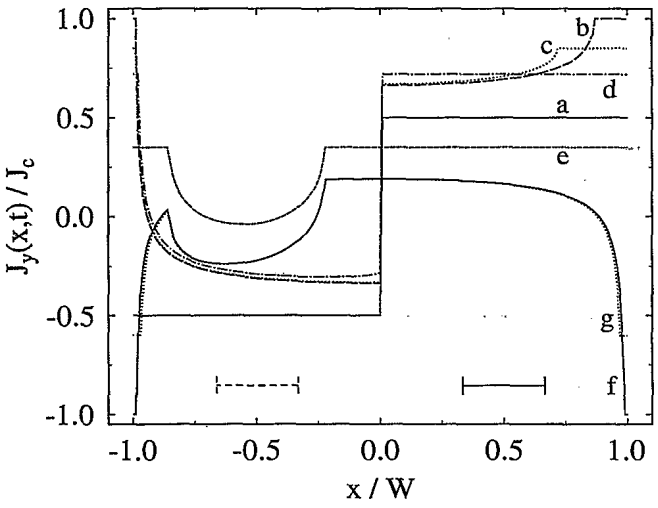

FIG. 4. The calculated reduced current density J_y/J_c flowing in a thin film superconductor as a function of position x for a transport current I_T applied in the y direction. The center of the film is at $x=0$, while the film edges are at $x/W=\pm 1$. Curve a corresponds to uniform relaxation to $|J_y|=0.5J_c$ after establishing the remanent critical state in the film. Curve b shows the effect of a transport current $I_T=0.25I_c$ applied to the relaxed state. Curve c shows the effects of relaxation a short time after current application, while curve d shows relaxation to the time $t=t^*$ (where $p+a=0$). Curve e shows relaxation for $t>t^*$ just prior to current removal. Curve f shows the effect of removing the current, while curve g shows the effects of relaxation a some time after transport current removal. Solid line at bottom of figure shows position and width of Hall sensor for positive transport currents, while the dashed line shows the equivalent position of the sensor for analyzing the effect of negative transport currents.

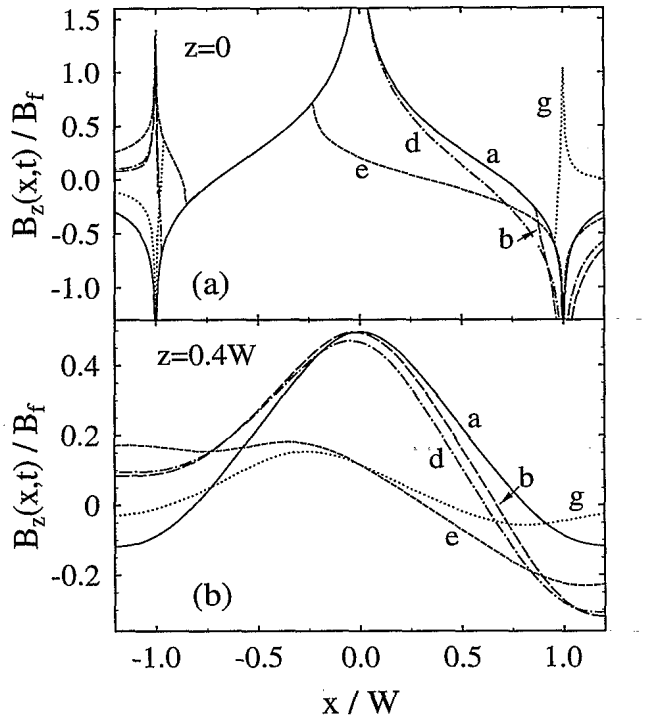

FIG. 5. (a) The calculated z component of the magnetic flux density $B_z(x)$ at the film surface as a function of position x and (b) $B_z(x)$ at a position 46 μm above the surface. The curves a through g correspond to the curves labeled similarly in Fig. 4. The field is normalized by using $B_f=4dJ_c/c$.

Using these relations and Eqs. (5) and (6), we may readily evaluate numerically the parameters a and p at any given time t. Curve c in Fig. 4 shows the effects of relaxation for $t>t_{\rm on}$.

Equations (4)–(6) hold as long as the right-hand edge of the field-invariant region is at $x>0$, namely $p+a>0$. At a particular time t^*, the right-hand edge of the field-invariant region reaches the center of the strip and $p+a=0$. Curves d in Figs. 4 and 5(a) show the current and field distributions at $t=t^*$. Outside the field-invariant region, the current density at t^*, $J_c^*(t^*-t_{\rm on})$, will be larger than $J^{\rm on}$ for any positive applied transport current. Hence, from Eq. (1) it follows that $t^*-t_{\rm on}<t_{\rm on}$, so that the described current distribution is obtained shortly after the transport current is applied. Since the relaxation is investigated experimentally on long time scales, most of the observed decay occurs at $t>t^*$, so that $p+a<0$. In this case the added current distribution $J_y'(x,t)$ is given by

$$J_y'(x,t)=\begin{cases} J_L(t), & -W<x\le p-a\ , \\ \dfrac{1}{\pi}\left[J_R(t)\arcsin\dfrac{(x-p)(W-p)-a^2}{a(W-x)}-J_L(t)\arcsin\dfrac{(x-p)(W+p)+a^2}{a(W+x)}\right. & \\ \quad\left.+[J_L(t)-J_R(t)]\arcsin\dfrac{(x-p)p+a^2}{ax}\right]+J_L(t), & p-a<x<p+a\ , \\ J_L(t), & p+a\le x<0\ , \\ J_R(t), & 0\le x<W\ . \end{cases} \tag{8}$$

The total current density is given by the superposition of $J_y(x,t_{\rm on})$ and the added current density $J_y'(x,t)$. As in the case of Eq. (4), the time-dependent parameters a and p are determined by the requirements that the total current is equal to the transport current I_T and the field B_z is invariant in the central region. These requirements yield

$$I_T = d[J_R(t)\sqrt{(W-p)^2-a^2}+J_L(t)\sqrt{(W+p)^2-a^2} + [J_L(t)-J_R(t)]\sqrt{p^2-a^2}] , \quad (9)$$

and

$$\frac{\sqrt{(W-p)^2-a^2}+W-p}{\sqrt{p^2-a^2}-p} = \left[\frac{\sqrt{(W+p)^2-a^2}+W+p}{\sqrt{p^2-a^2}-p}\right]^{J_L(t)/J_R(t)} . \quad (10)$$

The time decay of J_L and J_R is given by Eq. (7). Note that at $t>2t_{on}$, $J_R(t)$ becomes negative, which means that the total current density at $x>0$ has dropped below J^{on}, as shown by curve e in Fig. 4.

Curves e (short dash) in Figs. 4 and 5(a) show the current and field distributions at longer times just prior to the removal of the transport current at $t=t_{off}$. Removing the positive transport current I_T is equivalent to adding a negative current $-I_T$ to the current distribution that exists at t_{off}. The resulting current density profile is therefore a superposition of the total current distribution at t_{off} and the added current distribution $J_y''(x,t_{off})$ due to the negative transport current change. At $t=t_{off}$ the total current density on both edges of the film has dropped to a value $J^{off}=J_c^*(t_{off}-t_{on})$ given by Eq. (2). The available current density for the negative $-I_T$ is therefore J_c+J^{off}. The added current density at the edges will decay with time as $J_c^*(t-t_{off})+J^{off}$ with the resulting J_y'' given by

$$J_y''(x,t) = -\begin{cases} \frac{2}{\pi}[J_c^*(t-t_{off})+J^{off}]\arctan\sqrt{W^2-a^2/a^2-x^2}, & |x|<a , \\ J_c^*(t-t_{off})-J^{off}, & a\le|x|<W . \end{cases} \quad (11)$$

The new field-invariant region inside the film is symmetric with respect to $x=0$, and its time-dependent width $2a$ is now given by

$$a = W\left\{1-\left[\frac{I_T/2Wd}{J_c^*(t-t_{off})+J^{off}}\right]^2\right\}^{1/2} . \quad (12)$$

Curve f in Fig. 5 shows the total current density distribution immediately after the transport current is removed. Curves g in Figs. 4 and 5(a) show the effects of relaxation on the current and field distributions for $t>t_{off}$. Figure 5(b) shows corresponding curves of $B_z(x)$ that are calculated at the center of the Hall sensor at a distance z above the surface. The general features of the $B_z(x)$ profiles are similar, but there are some differences in detail. At finite heights there are no divergences of the field profile, and the sharp features are significantly rounded. In addition, the field B_z at a height directly above the field-invariant regions of the film does vary with time because the relaxing current distribution provides the required field invariance only in the plane of the film.

IV. CORRESPONDENCE OF DATA AND MODEL

Shown in Fig. 6 are the results of a calculation of the time dependence of B_z for the case of relaxation from the remanent magnetic state. The actual width of the Hall sensor employed in the experiment and its actual position were used in this calculation. Figure 6 shows the average $B_z^{av}(t)$ at the position of the Hall sensor, as relaxation initially takes place from the remanent critical state and is followed by application of either a positive or negative current of magnitude $|I_T|=0.05I_c$ at $t_{on}=100$ s, after which the current is removed at $t_{off}=2000$ s. In Figs. 4 and 5 we have shown only the results for the application of a positive transport current. By symmetry, application of a negative transport current gives rise to profiles that are a 180° rotation of those shown in Fig. 4 and the mirror image of those shown in Fig. 5. Therefore, in considering the negative current data, one should imagine having the Hall sensor moved from its actual position (Fig. 4, solid line) to a position equidistant form the opposite edge of the strip (Fig. 4, dashed line). It can be seen that the general features of the experimental results presented in Figs. 1 and 3 are reproduced by the calculation (Fig. 6). Application of a positive current results in a negative step at t_{on} accompanied by an increased relaxation rate that gradually approaches the baseline relaxation rate expected for the case when a transport current is never applied (Fig. 6, dashed line). Removal of the positive

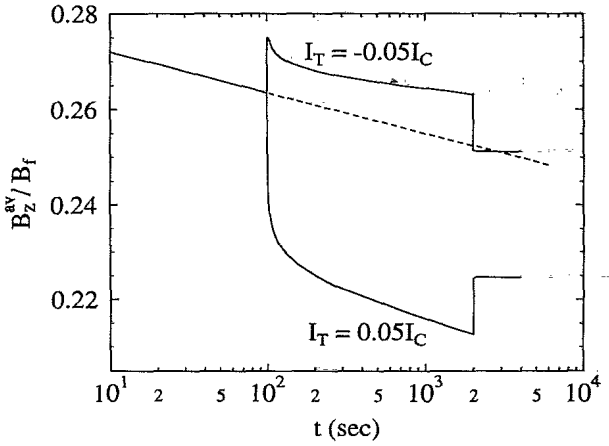

FIG. 6. Calculated time dependence of $B_z^{av}(t)$, the magnetic flux density averaged over the sensor cross section, when a transport current $I_T=\pm0.05I_c$ is applied to the remanent critical state at $t_{on}=100$ s and removed at $t_{off}=2000$ s. The dashed line represents the relaxation if a transport current is not applied (baseline relaxation). The parameters $t_c=10^{-10}$ s and $J_{th}/J_c=0.01$ were used in the calculation.

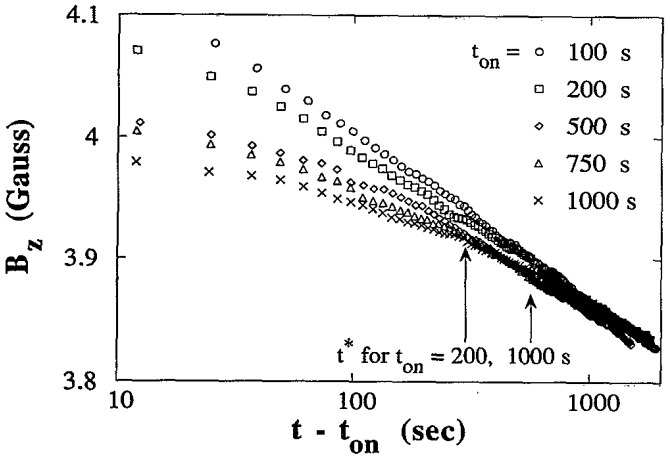

FIG. 7. Time dependence of the local magnetic flux density $B_z(t)$ as a function of $\log_{10}(t-t_{on})$ in the case of positive current application at different values of t_{on}. The vertical arrows identify the approximate values of t^* for $t_{on}=500$ and 1000 s.

current produces a positive step in B_z, and, most notably, B_z retains a large negative offset from the baseline value. Application of a negative current results in a positive step at t_{on}, accompanied by an increased relaxation rate that gradually approaches a relaxation rate much lower than the baseline relaxation rate. Removal of the negative current produces a negative step in B_z. However, now B_z has a value very close to the baseline B_z value. The calculation exhibits a significant reduction in the relaxation rate upon removal of either a positive or negative current.

The steps in B_z at t_{on} and t_{off} result primarily from finite separation of sensor and sample and from the finite size of the sensor. Rather than measuring the B_z immediately adjacent to the surface, as in Fig. 5(a), the sensor actually measures B_z at a height above the sample surface, as in Fig. 5(b).

The initial increase in the relaxation rate observed upon application of a positive current (Fig. 1) can be explained using Fig. 4. Curves *a* and *b* of Fig. 4 show the effects of applying a positive current. Prior to application of the transport current, the right-hand side of the sample ($0<x<W$) carries positive $J_y(x)$, while the left-hand side ($W<x<0$) carries a negative $J_y(x)$. Adding a positive transport current increases the total current density J_y on the right-hand side and decreases the average $|J_y|$ on the left-hand side. Therefore, the relaxation rate will be enhanced for $x>0$ and generally suppressed for $x<0$. These trends can be seen clearly in Figs. 1 and 3.

Figure 7 shows the relaxation of B_z after the application of a positive transport current for various values of t_{on}. Since application of the transport current essentially resets the clock for the relaxation of the time-dependent critical current density, these curves are shown as a function of $t-t_{on}$. In Fig. 7 it can be seen that there is a change in the relaxation rate that we associate with the time t^*. For short values of t_{on}, J_{on} is relatively high, and the time t^* required for the right-hand edge of the field-invariant region to reach $x=0$ is relatively short. At times $t=t_{on}$ larger than t^*, the relaxation rate approaches the baseline relaxation rate.

Upon removal of the current, the magnitude of the current density inside the film decreases on the average, causing much of the sample to have current densities well below J_c, thereby slowing down the rate of relaxation. This explains the reduced rate of relaxation for $t>t_{off}$ shown in Figs. 1 and 3.

V. SUMMARY

The effect of transport currents on the spatial dependence of the current density and the normal component of the magnetic flux density has been studied experimentally and modeled theoretically. The model of Refs. 2 and 3, which accounts for demagnetization effects, has been extended here to explicitly include a time dependence. A simplified account of the relaxation has been carried out by using a phenomenological time-dependent critical current density with a logarithmic relaxation rate. The main features of the experimental results have been reproduced by a calculation using this model with actual experimental parameters: Hall sensor size and position, applied transport current densities, and independently determined J_c values.

ACKNOWLEDGMENTS

We thank M. Indenbom for valuable discussions and M. Konczykowski for the Hall sensors. The work at Purdue University and Ames Laboratory was supported in part by the Director for Energy Research, Office of Basic Energy Sciences. The work at Purdue University was supported by the Midwest Superconductivity Consortium (MISCON) through DOE Grant No. DE-FG02-90ER45427. Ames Laboratory is operated for the U.S Department of Energy by Iowa State University under Contract No. W-7405-Eng-82. The work at the Weizmann Institute was supported by the Israeli Ministry of Science and the Arts.

[1]M. Konczykowski, F. Holtzberg, and P. Lejay, Supercond. Sci. Technol. **4**, S331 (1991).
[2]M. J. Darwin, J. Deak, L. Hou, M. McElfresh, E. Zeldov, J. R. Clem, and M. Indenbom, Phys. Rev. B **48**, 13 192 (1993).
[3]E. Zeldov, J. R. Clem, M. McElfresh, and M. J. Darwin, Phys. Rev. B **49**, 9802 (1994).
[4]E. H. Brandt, M. Indenbom, and A. Forkl, Europhys. Lett. **22**, 735 (1993).
[5]E. H. Brandt and M. Indenbom, Phys. Rev. B **48**, 12 893 (1993).
[6]E. H. Brandt, Phys. Rev. Lett. **71**, 2821 (1993); E. H. Brandt, Phys. Rev. B **49**, 9023 (1994).
[7]A. Gurevich and E. H. Brandt, Phys. Rev. Lett. **73**, 178 (1994).
[8]R. E. Muenchausen, K. M. Hubbard, S. R. Foltyn, R. C. Estler, and N. S. Nogar, Appl. Phys. Lett. **56**, 578 (1990).
[9]A. Gurevich and H. Kupfer, Phys. Rev. B **48**, 6477 (1993).